Dynamics of the Mixed Layers in Stratified Sheared Flows

Georgy Manucharyan

October 18, 2010

1 Introduction

Vast verity of geophysical flows occur in density stratified fluids in a presence of sheared mean velocity profiles. Under such conditions it's been observed that vigorous turbulence leads to generation of mixed layers within the fluid, e.g. the regions of homogeneous density separated from each other by strong density gradients (interfaces). These layers could be of large vertical scales as well as of fine scales. An example of such flows is the destratification of the upper layer of the ocean under the action of the surface wind stress and the formation of multiple mixed layers which are observed within the seasonal thermocline in the ocean as well as in fresh lakes [10]. Such structures in a turbulent flows are thought to play a crucial role in the determining the turbulent fluxes of momentum, buoyancy and other tracers which in turn affect the further dynamics of the flow. Nonetheless, the problem of turbulent transport remains one the most difficult ones in geophysics.

Previous studies investigated mechanisms acting in stratified turbulent flows - a review of those could be found in [4]. The formation of small scale mixed layers in stratified fluids driven by external mechanical sources of turbulence were investigated by theoretically by Balmforth et al [1], and experimentally by Park et al [6]. In the present study the dynamics of layers is explored within a turbulent fluid in a presence of a sheared mean flow. A set of experiments were performed in which a linearly stratified fluid is driven by the stress applied by a rotating horizontal disk at the surface. This setting leads to the formation of the surface mixed layer extending from the the disk into the interior of the fluid. Its evolution with time and its dependence of the stratification and the rotation of the disk are obtained. Furthermore, small scale mixed layers were observed in below the surface mixed layer. They have a complicated dynamics with multiple regimes, which were attempted to characterize. The description of the experiment and the behavior of the observed mixed layers is presented in section (2). Further, a phenomenological model is developed that explains the mechanism under which the secondary mixed layers are formed. It parametrized the action of the two mechanisms: shear generation of the turbulence due to Kelvin-Helmholtz type of instabilities, and the mean flow generated turbulence though the vortex scraping mechanism. The resulting gradient-type mixing model predicts the formation of the instabilities in a particular parameter regime that lead to mixed layers formation. The instabilities are related to those described by Phillips [7] and Posmentier [8]. The model description, its analysis and numerical simulations are presented in section (3). The summary of the work is in section 4.

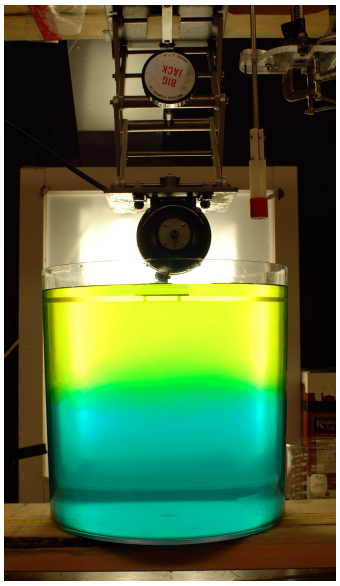

Figure 1: Experimental set-up: cylindrical tank filled with stratified fluid, rotating disk at the surface of the fluid, conductivity probe

2 Experiments

A series of experiments were made where a stratified fluid was forced by a rotating horizontal disk at the surface with the objective to investigate the dynamics of the formed mixed layers under various cases of stratification and the disk rotating speeds. The experimental setting is similar to that used by Davies et al [3], who investigated the flow generated during the spin up process and further established secondary circulation.

2.1 Experiment arrangement

Experimental set-up is shown on Figure 1. A cylindric tank of 30 cm height and 30 cm diameter was filled with a salt stratified water. Only linear stratifications were considered, which were obtained with a standard double bucket technique [5]. The range of density variations within the fluid was from 2% to 20%. A horizontal disk with the diameter of 24 cm is located at the surface of the fluid, with its axis of rotation aligned with the axis of the cylinder. The rotation speed of the disk is controlled by the motor (attached above the disk) that gives a range of 0.5 – 10 rad/s. Measurements of vertical density profiles were obtained using a conductivity probe which was taking 100 measurements per 1 cm of fluid, moving vertically with a speed of 3 mm/s. Measurements were taken only when the probe was moving down to avoid fluxes of water along the probe that would contaminate the data. The probe Reynolds number is of the order of 100 (this is an upper bound, which is reached at the edge of a disk); thus, measurements are not considerably affected by the presence of the probe on a scales considered in the current study - $O(cm)$. The profiled depth of the fluid was 20 cm, whereas the height of it is $27cm$. Density was calculated based on conductivity with a calibration using a 3rd order polynomial as a mapping function. To

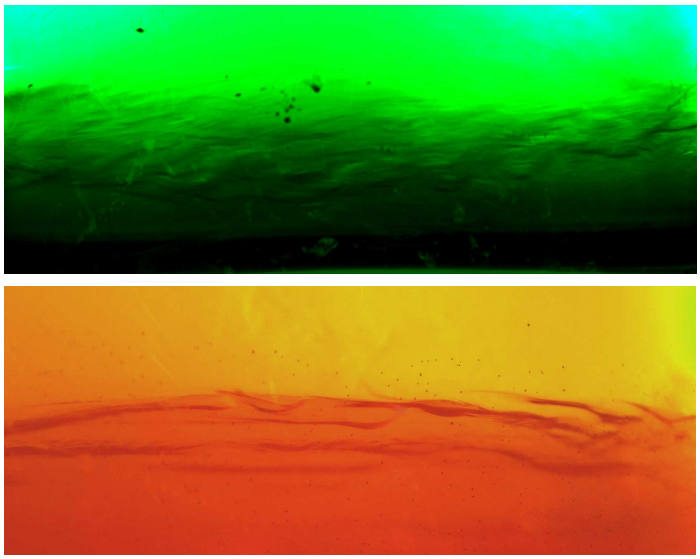

Figure 2: Images of the typical interfaces between the well mixed layer and a linearly stratified layer below it.

reduce temperature effects on conductivity the fluid allowed to reach the room temperature (20^oC) before the start of the experiment. Thus, the control parameters that define the outcome of the experiment were the stratification of the fluid (expressed as a Brunt–Väisälä frequency N) and the rotating speed of the disk Ω.

There are multiple non-dimensional parameters involved in current experiments. The most relevant one is the Richardson number, which will be defined here as $Ri = \frac{N^2}{\Omega^2}$. This definition should not be confused with the local Richardson number $\frac{N^2}{{U_z}^2}$ which varies with time and the location in the fluid. The explored range of $Ri \in (0.15 - 2.3)$. Another parameter would be the disk edge Reynolds number: $Re = \frac{UL}{\nu} \sim 10^5$, where U is the azimuthal velocity at the edge of the disk, L is the radius of the disk, and μ is the kinematic viscosity of water. A flow with such high values of Reynolds number could be considered turbulent and independent from the exact value of Re. The Schmidt number for the salt stratified water is $\sigma = \frac{\nu}{\kappa} \sim 700$, where κ is the salt diffusivity. The tank aspect ratio as well as the ration of the disk radius to the height of the water column is ~ 1. All geometrical parameters as well as the Schmidt number were fixed throughout all experiments. Thus, the only non-dimensional parameter that describes the different outcomes of the experiments is the Richardson number.

2.2 Observations of density profiles

After the tank is filled with the stratified fluid the disk is set in motion. As was mentioned previously, the disk Reynolds number is big enough that the flow adjacent to it becomes turbulent. Such flows are very effective in diffusing buoyancy and momentum. Thus, a mixed layer forms below the disk, with almost homogeneous density and velocity distributions. The growth of such a layer however is suppressed by the stable stratification of the

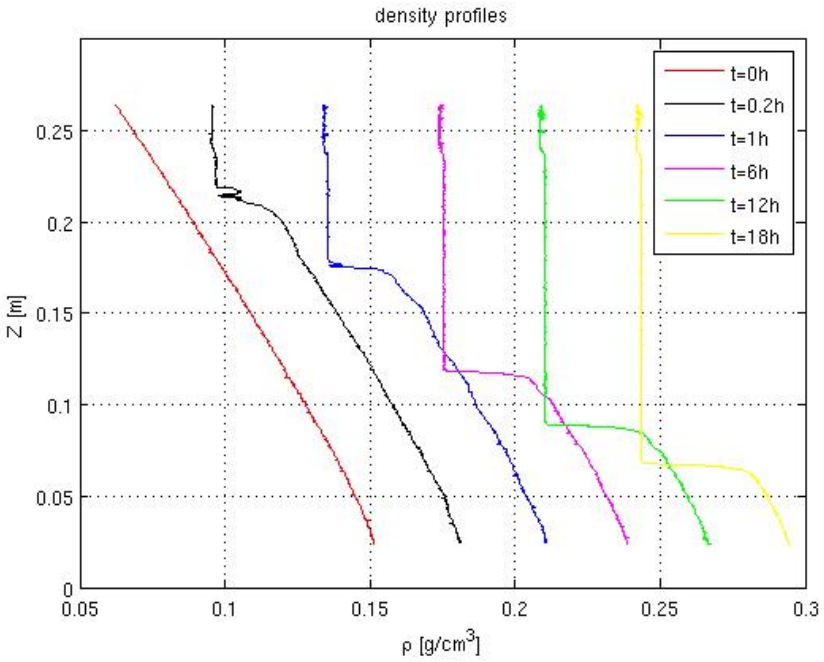

Figure 3: Density profiles plotted for different times after the start of the experiment. Profiles are shifted along the X-coordinate by $0.03 g/cm^3$ from each other.

fluid. As the mixed layer deepens the gravitational potential energy of the fluid increases because mixing process effectively lifts the center of the mass of a water column by mixing dense waters upwards against the gravitational field. Furthermore, mixing in a stratified fluid leads to formation of a density jump at the base of the mixed layer. The density jump suppresses turbulence and effectively separates the turbulent flow in the upper mixed layer from almost quiescent layer underneath it. Within the mixed layer there is a mean azimuthal flow due to the coherent rotation of the disk. This flow is also suppresses when it reaches strong stratification at the base of the layer creating a strong shear and providing other mechanisms of the generation of turbulence which would be discussed further.

Figure 2 shows images of two interfaces. The top one appears at early stages in the development of the mixed layer and is characterized by weak density jump across it, energetic eddies and large thickness (few cm). The one shown at the bottom, forms during later stages and has low energy eddies of smaller sizes (less then a cm) and much stronger density jump across it. The signature of these interfaces is clearly present in the vertical density profiles, the time evolution of which is shown on Figure 3. Initially, linearly stratified fluid get mixed from the top and forms a mixed layer as well as the density jump at the base of it, both of which are growing in magnitude. The interface separating the mixed layer from almost undisturbed bottom layer changes its characteristics as well. The profile taken at $t = 0.2h$ (hours) shows the presence of unstable stratification, which resulted from the overturning of energetic eddies at the base of the mixed layer. The density interface for this profile corresponds to a type shown on Figure 2 (top). At the profile taken at $t = 6h$ it is hard to see the density structures resulted from overturning of eddies because turbulence is

Exp#	N	Ω	Ri	α	A
9	0.5	1.13	0.2	0.2	0.42
13	0.5	1.34	0.14	0.18	0.5
14	0.52	0.72	0.52	0.2	0.32
15	1.37	1.7	0.65	0.23	0.27
17	1.3	0.95	1.87	0.246	0.19
18	1.1	1.5	0.54	0.22	0.29
19	1.12	1.7	0.43	0.2	0.36
20	1.18	1.13	1.09	0.25	0.21
21	1.3	1.34	0.95	0.24	0.23
22	0.98	0.95	1.05	0.24	0.24
23	0.84	2.08	0.16	0.21	0.46
24	0.78	0.72	1.18	0.24	0.23
25	1.46	1.13	1.67	0.25	0.18
26	1.7	1.7	1	0.225	0.22
27	1.7	1.13	2.25	0.225	0.24
28	1.72	3.14	0.3	0.18	0.41
29	1.6	1.94	0.67	0.22	0.29
30	1.42	1.13	1.57	0.23	0.22
31	1.5	1.18	1.6	0.24	0.22
32	0.94	1.5	0.4	0.23	0.29

Table 1: The table shows the experiment settings: initial stratification of the fluid (N), the disk angular velocity Ω. The last two columns show the coefficients of the power law fit for evolution of the mixed layer depth $\hat{h} = A\hat{t}^{\alpha}$. The values are organized and sorted by the experiment number.

highly suppressed there and eddies are of smaller scale; this interface corresponds the one on Figure 2(bottom).

The presence of the density jump and a velocity shear across it points to a possibility of generation of the Kelvin-Helmholtz type of instabilities at the interface that leads to its further erosion. However, these type of instabilities would be present if the local Richardson number ($N^2/{U_z}^2$) is sufficiently small. Eventually the flow would reach conditions stable to K-H instabilities as the velocity of the mixed layer would gradually slow down, whilst the density jump across the interface would increase. At this point, the erosion of the interface would continue due to the mean flow acting frictionally on turbulent eddies at the interface (vortex scraping). Thus, whether it's the mean flow or its shear, there is a mechanism which would generate mixing at the stable interface and lead to its further deepening.

2.3 Development of the primary mixed layer

As was described earlier, a mixed layer forms at the disk and expands into the fluid reaching the thickness of the order of the tank size. It will be referred to as the primary mixed layer. In certain cases, there are other layers that form below it (secondary mixed layers) which

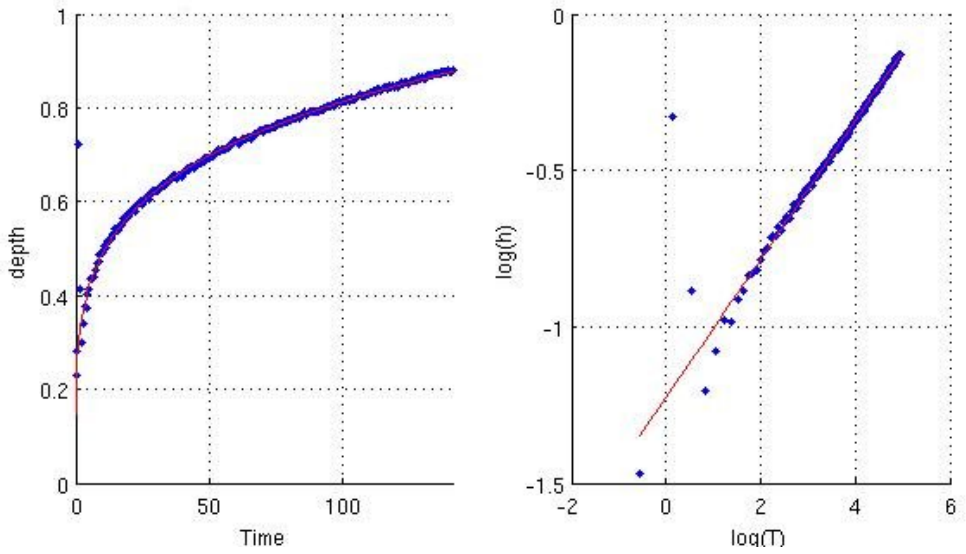

Figure 4: A non-dimensional depth of the primary mixed layer is plotted as a function of non-dimensional time (left) and on a log-log plot (right).

are of smaller scales and have much weaker interfaces. These will be discussed in the next section.

For many geophysical applications it is important to know the growth of the primary mixed layer with time as it controls the distribution of tracers as well as the dynamics of the flow . To present the observations, the mixed layer depth h is non-dimensionalized by the depth of the fluid ($\hat{h} = h/H_w$), and time t by the period of rotation of the disk ($\hat{t} = \Omega t$). Figure 4(left) shows the time evolution of the primary mixed layer for a typical experiment: the layer grows rapidly at first, then the growth slows down due to the increasing density jump at the base of the layer. Figure 4(right) shows the thickness of the layer as a function of time on a log-log plot with a corresponding linear fit ($R^2 = 0.89$). This fit suggests a power law $\hat{h} = A\hat{t}^{\alpha}$, where A and α presumably are functions of the Richardson number - the control parameter of the experiment. Indeed, Figure 5 shows that there is a particular dependence of the fit coefficients on the Richardson number. The power α stays relatively constant at a value of 0.22 with some trend towards smaller values at lower Richardson numbers. The coefficient A of the fit seems to scale with the Richardson number as $A \sim Ri^{-0.33}$ as shown in Figure 5(right). Thus, the experimental data shows that the non-dimensional mixed layer depth scales as $\hat{h} \sim Ri^{-0.33}\ \hat{t}^{0.22}$.

To understand the obtained dependence of the mixed layer depth evolution, consider the energy balance of the system. The source for the generation of the mean flow as well as the mixing of the stratified fluid is a power produced by frictional stress due to motion of the disk. It scales as $P \sim \tau U \sim U^3$, where $\tau \sim U^2$ is the frictional stress and U is the characteristic velocity of the mixed layer near the disk. Further, a linearly stratified fluid that was mixed to a depth h would have its gravitational potential energy increased by $\Delta GPE = \int_{-h}^{0}(\rho - \rho_0)gzdz \sim N^2h^3$, where ρ_0 is the initial linear density profile and ρ is the one obtained by adiabatic mixing the initial profile within the layer of thickness h. At last,

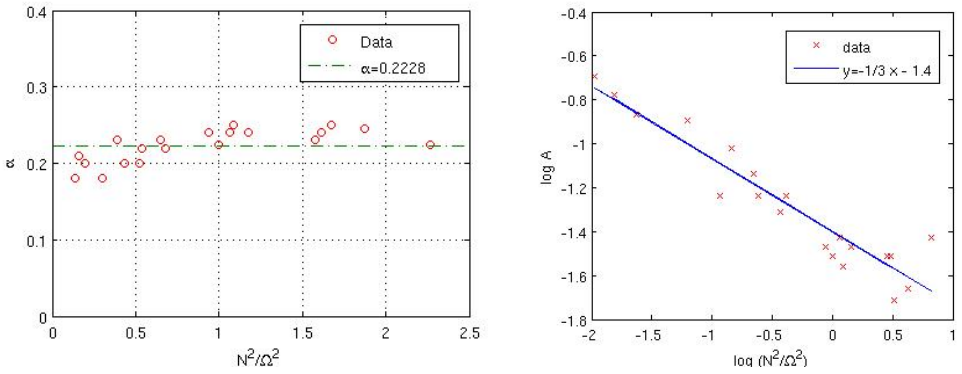

Figure 5: Coefficients of the power fit for the depth of the mixed layer are plotted as functions of Ri. On the left is the coefficient $\alpha = \alpha(Ri)$; coefficient $A = A(Ri)$ plotted on a log-log scale (right).

the kinetic energy of the mixed layer would scale as $KE \sim U^2 h$ and the dissipation D is assumed to be proportional to the energy production ($D = \gamma P$). Thus, the energy balance is described by the following equation:

$$\frac{d}{dt}(KE + PE) = P - D \Rightarrow \frac{d}{dt}(U^2 h + N^2 h^3) \sim U^3$$

At this point, an assumption is made that the flow reaches a state where the kinetic energy of the mixed layer approaches a constant value and the energy input redistributes between potential energy and dissipation. If $KE = cont$ then $U \sim h^{-1/2}$ and the energy balance model becomes $h^2 h_t \sim h^{-3/2} \Rightarrow h \sim t^{2/9}$. The obtained power law for the growth of the mixed layer is consistent with observations since they indicate a power of 0.22 (Figure 5). The dependence of the fitted coefficient $A \sim Ri^{-1/3}$ suggests that the assumed constant value of the kinetic energy is a function of Ri as well. This relation, could not be determined based on the simple energy balance model. The assumptions made in constructing an energy balance could be verified with measurements of the velocity of the fluid using, for example, PIV techniques. In current experiment these measurements were not produced, but for further progress there are of vital importance.

2.4 Dynamics of a secondary mixed layer

Layers of weak stratification that form below the primary layer will be referred to as the secondary mixed layers. Figure 6 shows an example of a developed secondary mixed layer - it has a distinct signature in density profile as well as in Brunt–Väisälä frequency, where bases of layers (interfaces) have strong stratification and the layer itself is weekly stratified. Thus, on Figure 6(right) the strong peak[1] corresponds to the base of a primary mixed layer, and the peak with smaller magnitude corresponds to the base of a secondary mixed layer.

[1]Buoyancy frequency was obtained from smoothed density profile to remove noise - instrumental as well as due to small scale overturning. This leads to broader peaks with smaller magnitudes; nonetheless, a clear signature of mixed layers is preserved.

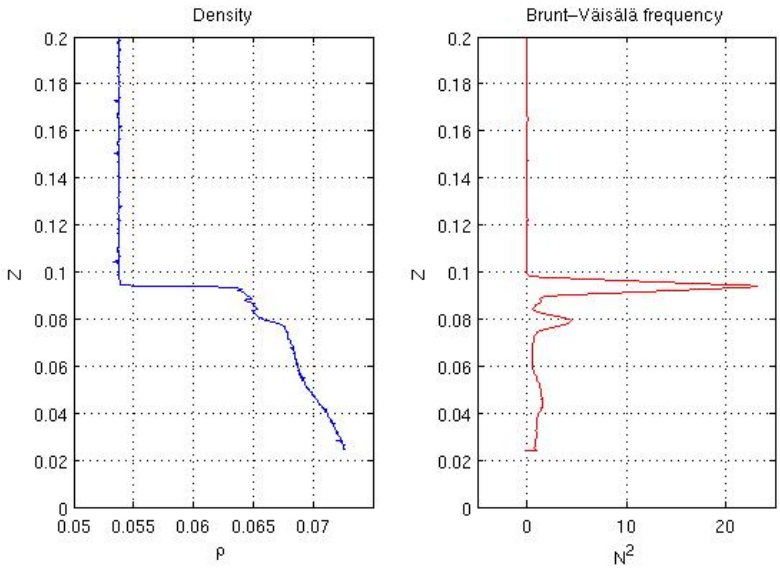

Figure 6: A typical density profile containing a primary mixed layer as well as a secondary one (left).Brunt–Väisälä frequency showing peaks at the bases of mixed layers.

Note that, secondary mixed layer is only partially mixed as apposed to the primary one that is completely destratified. Thus, secondary layers are characterized by the magnitude of a peak in buoyancy frequency at the base of the layer, and by a layer thickness, which is the distance between the two peaks.

As opposed to primary mixed layer, that monotonically grows with time, the secondary layer has a very rich dynamics. Figure 7 shows how the buoyancy frequency evolves with time. Here, there is a clear indication of both mixed layers - the primary one continuously grows and the secondary one forms and decays multiple times throughout the experiment. Characteristic thickness of the secondary layer is of few centimeters. The evolution process could be decomposed in several stages. In the beginning, there is a strong turbulent flow that drives the growth of the primary layer and does not allow the formation and persistence of the fine scale secondary layer. Then follows a period of time when the secondary layer forms and decays with a characteristic time of few tens of minutes. The layer forms spontaneously having a finite thickness which then decreases until this layer merges with the primary one (collision instability) and the process repeats. The next stage is described by a change in the way the layer forms. They appear at the base of a primary mixed layer having small thickness and start to grow building up the density jump at the interface. However, the magnitude of a jump vanishes with time (erosion instability), the layer disappears and the next one forms. Finally, comes the stage when the layers either no longer form or stay in a locked position relative to the primary interface.

The evolution of the secondary mixed layer is highly dependent on the Richardson number for the experiment and in a current time. In some cases, certain stages of the evolution could be skipped which makes it hard to classify all the regimes. Nonetheless, an attempt to plot a regime diagram was made. Figure 8 shows the stages of the evolution of the mixed layer for different experiments as a function of non dimensional time and

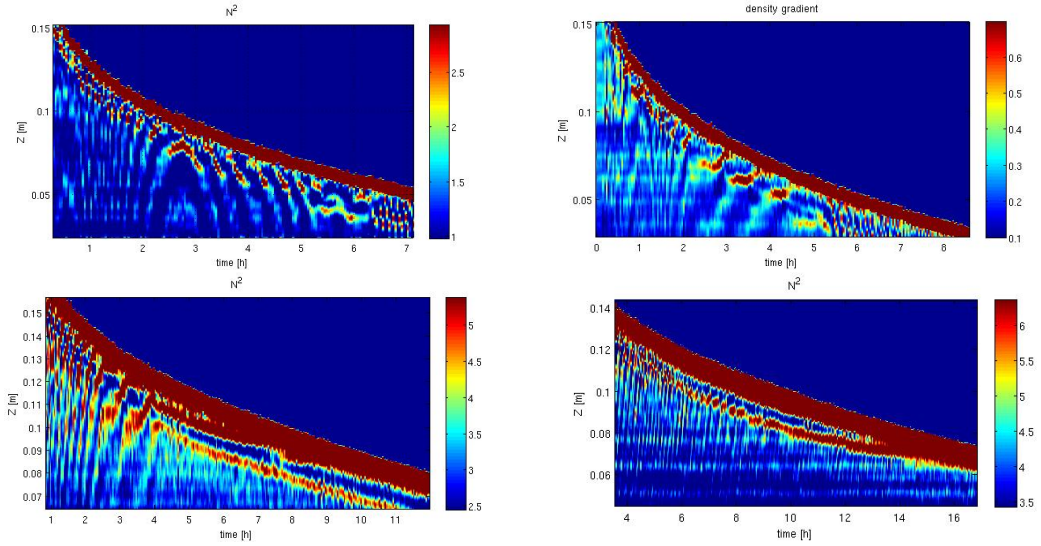

Figure 7: Examples of the time evolution of the square of the Brunt–Väisälä frequency for different values of the Richardson number ($Ri = 0.54, 1, 2.25, 1.67$).

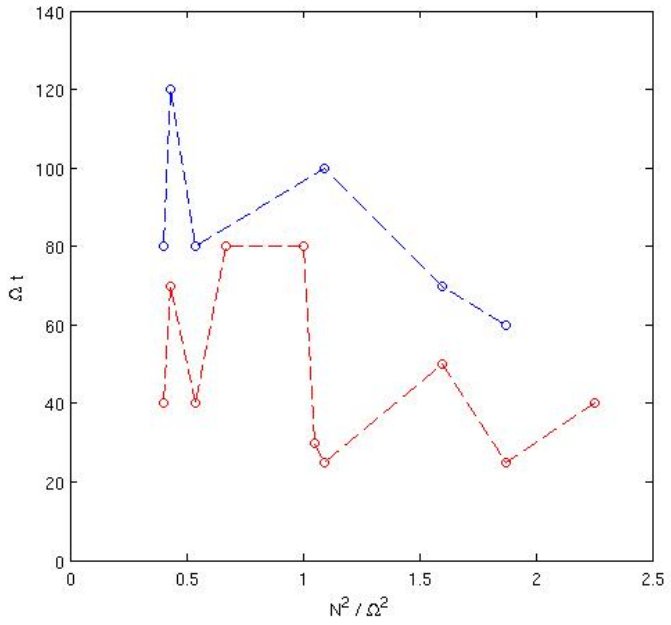

Figure 8: Regime diagram showing different stages of evolution of the secondary mixed layer

Richardson number. Below the red curve steps generate below the mixed layer and decay by merging, whereas in between the red and blue curves mixed layers generate from the primary mixed layer and decay by erosion. Above the blue line the staircases are either in locked state or do not exist. The diagram does not show any specific dependence, however this does not imply that there is no dependence whatsoever. There is an obvious lack of data: a total of 20 experiments were made and for less then half of them the secondary mixed layers could be clearly classified. Furthermore, since there are no theoretical predictions it is not clear how to present such a diagram: the most obvious choice of presenting in terms of Richardson number and time might not be the clear one to look at.

The dynamics of the secondary mixed layers is extremely complicated. Understanding it to a level of making predictions requires a precise theoretical model bucked up by extensive observations of not only density but also velocity fields, turbulent buoyancy and momentum fluxes. However, due to time constrains these elaborate measurements could not be performed. Thus, the theoretical part of this research would be focused on explaining the formation of secondary layers in an idealized phenomenological framework.

3 Phenomenological model

Secondary mixed layers arise in a stratified fluid that is subjected to the action of a turbulent flow with a mean shear. The turbulent nature of the flow would be the key to understanding the phenomenon. The proposed mechanism is as follows. The sheared mean flow driven by the rotating disk is a source of turbulent motion which inhomogeneously distributes within a stratified fluid depending on its stratification. The buoyancy itself is affected by turbulent fluxes. Thus, the formation on the layers could be related to the instability of the turbulent flux-buoyancy relation as was first proposed by Phillips [7] and Posmentier [8]. Suppose, the evolution of buoyancy b is controlled by the divergence of the downward turbulent buoyancy flux F:

$$\frac{\partial b}{\partial t} = \frac{\partial F}{\partial z}$$

and this flux is a function of the buoyancy gradient $F = F(b_z)$. The equation has obvious steady state solutions with constant flux, however such solutions would be unstable if the flux would be a decreasing function of buoyancy gradient e.i. $\frac{\partial F}{\partial b_z} < 0$. Figure 9 shows the mechanisms of the instability. A linear steady state buoyancy profile (dashed line) has a value of buoyancy gradient that corresponds to the negative derivative of the buoyancy flux. After introducing a small perturbation (black line) there will appear anomalous buoyancy fluxes (blue arrows). In regions where the perturbations have higher buoyancy gradient the anomalous flux is negative and in it is positive in regions of lower gradients. As could be seen from the evolution equation the current distribution of the buoyancy fluxes would lead to a growth of the initial perturbation, meaning that the base state is unstable. This instability would lead to buoyancy profiles consisting of a series of mixed layers separated by strong interfaces (staircases). In the case of $\frac{\partial F}{\partial b_z} > 0$ the created fluxes would lead to the decay of the buoyancy anomaly - this state is stable.

This model considers the buoyancy equation only and assumes a particular shape of the flux-gradient curve. However, the exact form of this curve would depend on particular mixing mechanisms that create the turbulent buoyancy fluxes. In the following section

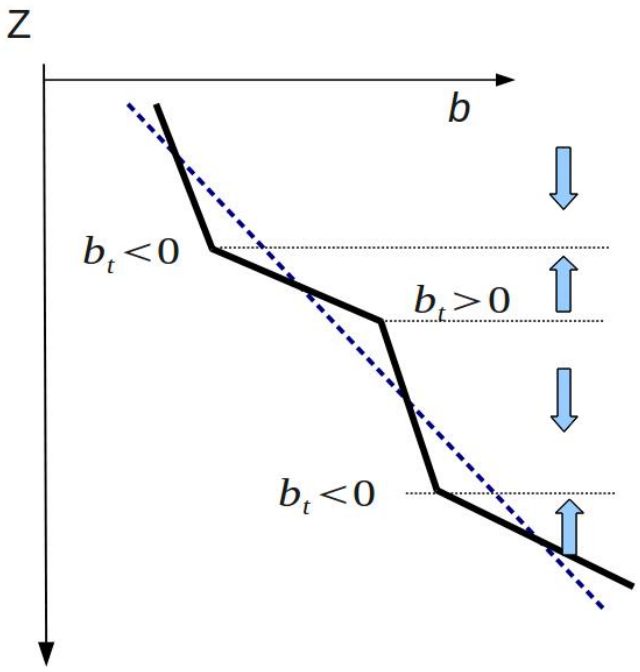

Figure 9: Schematic representation of the instability mechanism that leads to layer formation. Dashed line represents the initial buoyancy profile, black line is the slightly perturbed profile, anomalous buoyancy fluxes denoted by blue arrows.

a gradient-type mixing model would be devised that would describe the development of buoyancy profiles under the action of the mean flow generated turbulence. The formation of the layers in the model would be related to the mechanism described above by calculating the exact form of the flux-gradient relation. The model would consist of evolution equations written for buoyancy as well as for turbulent kinetic energy that is drained from the mean flow. It is aimed to describe the secondary mixed layers only, so it is assumed that the primary layer has been formulated and the mean velocity profile is established.

3.1 Model formulation

The approach taken in constructing a mixing model is similar to that implemented by Balmforth [1] and Barenblatt [2]. The model parametrizes turbulent vertical transports as gradient transports using eddy diffusivity and viscosity. Thus, the conservation laws for horizontally averaged buoyancy b and turbulent kinetic energy e are as follows

$$\frac{\partial b}{\partial t} = \frac{\partial}{\partial z}(\kappa \frac{\partial b}{\partial z}) \quad (1)$$

$$\frac{\partial e}{\partial t} = \frac{\partial}{\partial z}(\kappa \frac{\partial e}{\partial z}) + S \quad (2)$$

where S is a source term for the energy and κ is the turbulent diffusivity. The source term represents production and destruction of the turbulent energy and in this formulation

would consist of four terms:

$$S = -\kappa b_z - \alpha\frac{e^2}{\kappa} + \frac{1}{1+Ri}\kappa {U_z}^2 + \frac{Ri}{1+Ri}U^2 e^{1/2} l^{-1} \tag{3}$$

As it was mentioned previously, the mixing of buoyancy leads to an increase in a gravitational potential energy of the system. Thus, the role of the first term ($-\kappa b_z$) is to convert the eddy kinetic energy into potential energy preventing the artificial accumulation of the total energy $E = \int_0^H (e - bz)dz$. The second term $-\alpha\frac{e^2}{\kappa}$ is the dissipation, which is on dimensional grounds proportional to the energy e and to the inverse of the eddy turnover time $\tau \sim \kappa/e$; α is a small parameter which controls the intensity of the dissipation and effectively defines the number of turnover periods over which an eddy would dissipate. The last two terms are the production terms due to the action of a mean flow. From visual observations of the experiments there seem to be two mechanism in action. At low local Richardson numbers ($Ri = N^2/{U_z}^2$), where the destabilizing effect of the shear is dominating the stabilizing effect of the stratification, the turbulence is generated due to Kelvin-Helmholtz type instabilities. These instabilities, however, are suppressed at high Ri. Hence the representation of the energy production is of the form $\frac{1}{1+Ri}\kappa {U_z}^2$. At high Ri the turbulence is generated by the mean flow acting on turbulent eddies (vortex scraping) by inducing a frictional stress. The amount of power introduced by such a mechanism is proportional to $U^2 e^{1/2} l^{-1}$, where U^2 is scaling for the stress exerted by the mean flow, $e^{1/2}$ is a characteristic velocity of an eddy and l is its length scale. Factors $\frac{Ri}{1+Ri}$ and $\frac{1}{1+Ri}$ are chosen to ensure that the two mechanisms would act in their corresponding regime of Richardson numbers.

Eddy diffusivity, as well as viscosity, is[2] proportional to $le^{1/2}$. To close the system the characteristic eddy size l needs to be defined. Since the model aims to describe mixing in the stratified fluid there are several length scales involved. In the limit of strong stratification the size of eddies would be proportional to the Ozmidov's length scale $(e/b_z)^{1/2}$. This restriction comes from the fact that eddies overturn density layers leading to increase in potential energy. Thus, for a given energy of an eddy and the ambient stratification there would be a restriction on its size. In the limit of weak stratification, the characteristic length scale for an eddy $l = d$ should be related to the geometrical parameters e.i. the size of the tank[3]. Thus, to interpolate the two length scales in the limits of strong and weak stratifications expression for the eddy length scale l is chosen to be

$$\frac{1}{l^2} = \frac{1}{d^2} + \gamma\frac{1}{e/b_z} \tag{4}$$

where γ is a parameter that determines the length scale in the limit of strong stratification. It should be pointed out that the model is written in terms of locally defined dynamical variables, meaning that all the scales are controlled by the local dynamics and do not depend on global profiles of the variables. However, this doesn't always take place in reality. For example, the model used for the eddy length scale states that in the case of locally weak stratification the length should be equal to d - some geometrical restriction. However, vertical profiles of stratification containing mixed layers bounded by strong stratification

[2]For simplicity eddy viscosity and diffusivity are taken to be the same, however this assumption could be relaxed

[3]A restriction of the length scale in weakly stratified case avoids singularities in the model.

would impose an equivalent 'geometrical' constrain on an eddy size in the location within the mixed layer - the eddy size could not be greater than the thickness of a mixed layer with strong interfaces. Thus, the parameter d should be considered as effective one that takes into account geometrical constrains as well as the global buoyancy profile. In the current model, for simplicity it is assumed to be constant.

A resulting model is effectively a set of coupled nonlinear diffusion equations, which require boundary and initial conditions to be completed. As boundary conditions, the fluxes of energy and buoyancy are set to be zero at the top and the bottom boundaries of the domain e.i. $e_z = 0, b_z = 0$ at $z = 0, H$. The initial conditions would be discussed in a section 3.3. Thus, the complete equation set of the mixing model is the following:

$$
\begin{aligned}
b_t &= (\kappa b_z)_z && (5)\\
e_t &= (\kappa e_z)_z - \kappa b_z - \alpha\frac{e^2}{\kappa} + \frac{1}{1+Ri}\kappa {U_z}^2 + \frac{Ri}{1+Ri}U^2 e^{1/2} l^{-1} && (6)\\
\kappa &= l e^{1/2} && (7)\\
\frac{1}{l^2} &= \frac{1}{d^2} + \gamma\frac{1}{e/b_z} && (8)\\
Ri &= \frac{b_z}{{U_z}^2} && (9)
\end{aligned}
$$

where α, γ, d are fixed parameters; characteristic velocity U and velocity shear U_z represent the forcing for this system and assumed to be constant. In principle, equations 6 to 9 could be combined to give an evolution equation for the turbulent diffusivity κ - the variable that determines the evolution of the buoyancy profile.

Since the purpose of the model is to describe the formation of mixed layers it is convenient to use the buoyancy gradient ($g = b_z$) instead of buoyancy as a dynamical variable. The mixed layers would have a distinct signature in buoyancy gradient profile: low values within the mixed layer and sharp peaks at the interfaces. Further, it is useful to use non-dimensional equation set with the following definition of dimensionless quantities:

$$
\hat{t} = \frac{Ut}{\gamma d}, \quad \hat{z} = \frac{z}{\gamma^{1/2} d}, \quad \hat{e} = \frac{e}{U^2} \quad \hat{g} = g\frac{\gamma d^2}{U^2}, \quad \hat{l} = \frac{l}{d}, \quad Q = (\frac{U}{U_z d})^2 \qquad (10)
$$

In dimensionless form the equations are

$$
\begin{aligned}
g_t &= (\kappa g)_{zz} && (11)\\
e_t &= (\kappa e_z)_z - \kappa g - \alpha\gamma\frac{e^2}{\kappa} + \frac{\gamma\kappa + Q g^{3/2}}{1 + g/\gamma} && (12)\\
\kappa &= \frac{e}{(e+g)^{1/2}} && (13)\\
b.c. &: \quad e_z = 0, g = 0 \ at \ z = 0, H && (14)
\end{aligned}
$$

where a parameter Q describes the relative importance of the mean flow and the mean shear in the energy production term; the local Richardson number is proportional to the buoyancy gradient only ($Ri = g/\gamma$).

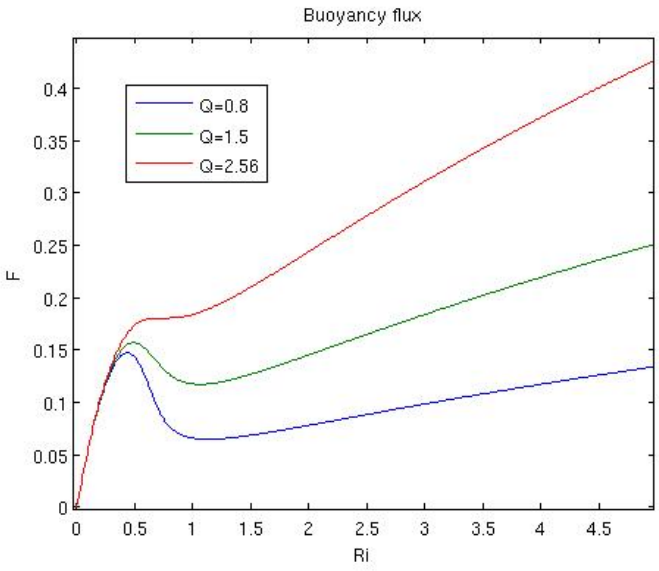

Figure 10: Steady state buoyancy flux plotted as a function of the buoyancy gradient for different values of the forcing parameter Q.

3.2 Steady states and their stability

Consider a steady state of the model, which has a constant energy and buoyancy gradient $(e_0, g_0) = const$. It violates the boundary conditions, nonetheless away from the influence of the boundaries it is useful to consider its stability. Such steady states should have no production of turbulent kinetic energy ($S = 0$) in order for dynamic variables not to change with time:

$$-\kappa_0 g_0 - \alpha\gamma \frac{e_0^2}{\kappa_0} + \frac{\gamma\kappa_0 + Q g_0^{3/2}}{1 + g_0/\gamma} = 0 \tag{15}$$

$$\kappa_0 = \frac{e_0}{(e_0 + g_0)^{1/2}} \tag{16}$$

This sets a constrain, which effectively defines energy and buoyancy flux as a function of buoyancy gradient (or Richardson number) for the considered steady state solutions:

$$e_0 = E(g_0) \tag{17}$$

$$\kappa_0 g_0 = F(g_0) \tag{18}$$

As was discussed earlier, the instabilities would develop if the initial profile has the Richardson number which is within the range of the negative slope of the buoyancy flux. Figure 10 shows the steady state buoyancy flux as a function of Richardson number ($Ri = g/\gamma$). The numerical values of parameters are chosen as $\alpha = 0.1, \gamma = 0.2$. The representative mean flow parameter $Q = 0.8, 1.5, 2.56$. Curves with values of $Q < 2.56$ show a non-monotonic behavior, having a region where the derivative of the flux is negative. At low

values of Ri, the instabilities are not possible due to extremely high turbulent energy created by shear instabilities that are not suppressed by the stratification. At high Richardson numbers the buoyancy flux is controlled by the turbulence produced by the mean flow which is proportional to $g^{1/2}$, hence the increase of the buoyancy flux with the increase in stratification. However, the shear production term is $\sim e/g^{3/2}$, which means that there is strong penalty in energy production for an increase in stratification - hence the turbulent flux due to shear production should decrease with the stratification at high Richardson numbers. Thus, the effect of the mean shear tends to destabilize the system and create mixed layers, whereas the mean flow turbulence has a stabilizing effect. Hence, in the intermediate range of Richardson the slope has a negative slope due to shear production term, however this region is of finite size due to the action of the mean flow turbulence at higher values of Ri. This means that the instability could not grow unbounded in time: at some point the effect of the mean flow turbulence would suppress the growth. Thus, the existence and development of instabilities depend crucially on the relative importance of the mean flow to shear production terms which is determined by the value of the parameter Q. If the forcing Q is greater than 2.56 the flux-gradient curve monotonically increases with the value of Richardson number - stabilizing effect of the mean flow is dominant. For such forcing all the buoyancy profiles would be stable.

The described instabilities could now be identified from the formulated model equations and their growth rates could be quantified. Linearizing the equations around the base state (e_0, g_0) and assuming exponentially growing solutions for perturbations $(\hat{e}, \hat{g}) \sim exp(\lambda t - ikz)$ leads to a linear stability problem:

$$\lambda \begin{pmatrix} \hat{g} \\ \hat{e} \end{pmatrix} = \begin{pmatrix} -k^2 f_g & -k^2 f_e \\ S_g & -k^2\kappa + S_e \end{pmatrix} \begin{pmatrix} \hat{g} \\ \hat{e} \end{pmatrix}$$

where $f = \kappa g$ is the buoyancy flux, S is the source term in the energy equation and all the partial derivatives are calculated at the point (e_0, g_0). Thus, for a given value of parameter Q and initial value of the Richardson number a growth rate λ could be calculated as a function of the wavenumber k. Figure 11 shows growth rates calculated for $Q = 1.5$ and for values of base state $Ri = 0.3, 0.7, 1.3$. The growth rate is positive for $Ri = 0.7$ which is located at the negatively sloped part of the flux curve (Figure 10). The growth rate is negative for the values of Richardson numbers of 0.3 and 1.3 that belong to the monotonically increasing part of the slope - these are stable solutions. An important property of the written model is that in the case of the unstable steady states the growth rate of the perturbations has has a high wavenumber cutoff[4] which means that small scale perturbations do not grow with time - instead, they decay. This property allows to perform direct numerical simulations of the development of the instabilities and their evolution leading to the formation of the mixed layers.

3.3 Numerical simulations

Numerical simulations of the mixing model were performed using first order in time and second order in space numerical scheme with an adaptive time stepping. Computational domain is $z = [0, 1200]$ having 600 uniformly distributed grid points. Initial conditions for

[4]The high wavenumber cutoff is due to the diffusion of the turbulent kinetic energy

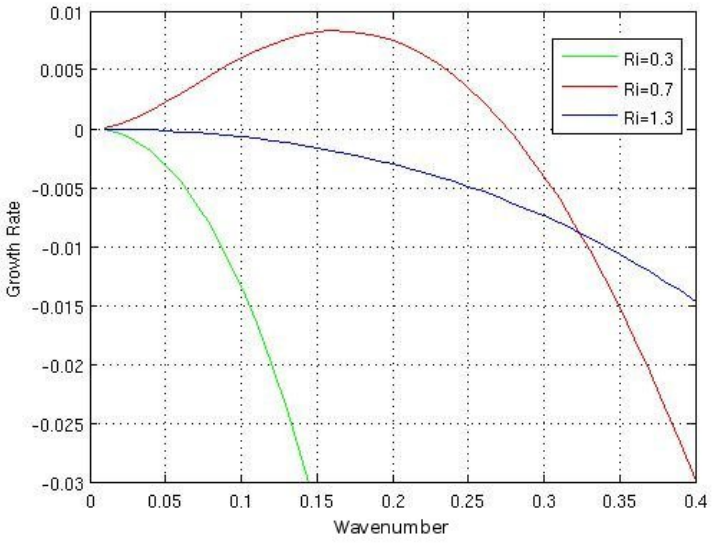

Figure 11: Growth rate plotted as a function of the wavenumber for different values of the base state Richardson numbers and for a fixed parameter $Q = 1.5$ (as predicted by the linear stability analysis).

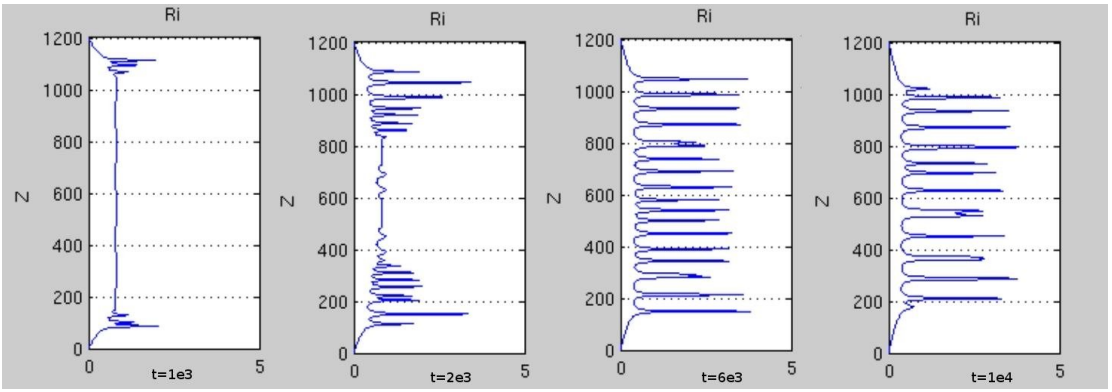

Figure 12: Numerically simulated evolution of the instabilities manifested in the vertical profiles of the Richardson number.

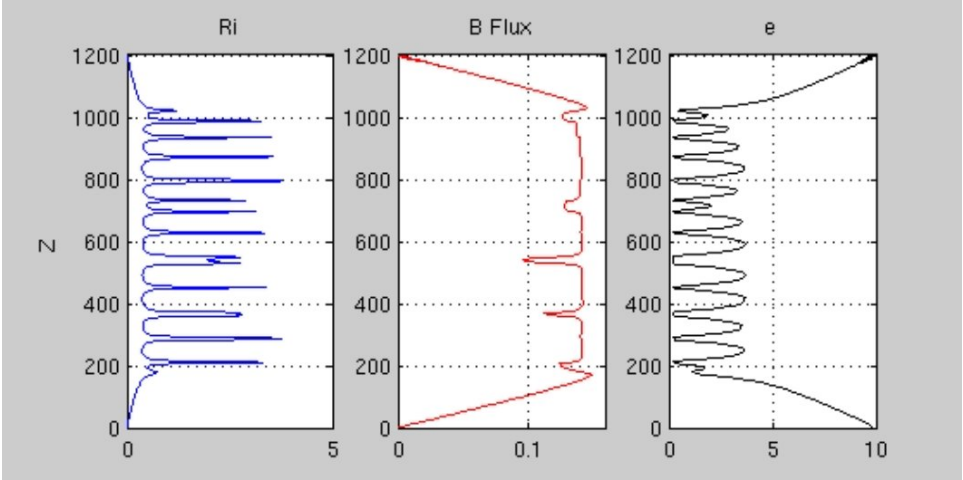

Figure 13: A snapshot of model variables at $t = 1e4$: Richardson number (left), buoyancy flux (middle) and turbulent kinetic energy (right).

the numerical simulation are chosen to be $Ri = 0.8$ for the buoyancy profile[5], $e = 0.01$ for the turbulent kinetic energy and the forcing parameter $Q = 1$. Based on a linear stability analysis such a configuration should be unstable. Indeed, the numerical simulations confirm it. Figure 12 shows snapshots of the modeled buoyancy gradient at different time - it is clearly seen that the instabilities are developing in the form of sharp peaks in buoyancy gradient profiles. First, the instabilities develop close to boundaries because there are larger perturbation from the steady state their. Then, they appear in the interior and eventually fill the whole domain except for small regions adjacent to boundaries which are affected by zero flux boundary conditions.

Figure 13 shows a snapshot of the buoyancy gradient g, turbulent kinetic energy e and a corresponding buoyancy flux f. The buoyancy flux seems to be relatively constant in the interior region, however having isolated regions of low flux. The energy distribution is higher in the regions of weak stratification and has minimums at within highly stratified interfaces. The instabilities develop having a wavelength corresponding to the one that has a maximum growth rate predicted by a linear stability analysis. However, it has been observed that after the initial development stage the structure tends to coarsen with time by merging or decaying mechanisms. The individual peaks are quasi-steady solutions of the equations and evolve by weakly interacting with each other. The result of the interaction could be considered as a secondary instability that leads to the coarsening through erosion or collision of the adjacent interfaces [9]. The time scales for the two instabilities would depend on the base.

Figure 14 shows the time evolution of the buoyancy gradient and the buoyancy flux throughout the whole simulation. The initial development stage lasts till the time $t \approx 4000$ and is characterized by the formation of the peaks in buoyancy gradient. The overall structure, however, tends to coarsen. The peaks either merge with each other creating a

[5]To satisfy initial conditions at the boundaries the distribution of Ri was chosen such that it is constant within the interior of the domain and continuously approaches zero at the boundaries.

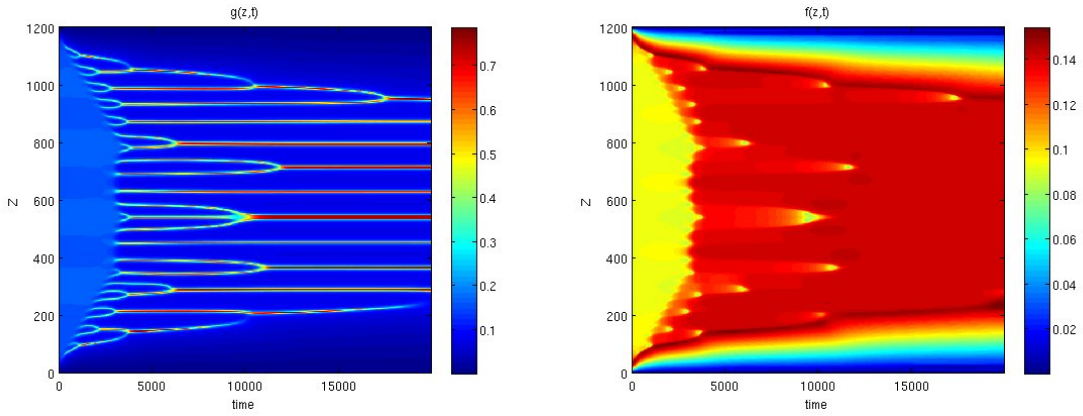

Figure 14: Time evolution of the modeled vertical profiles of the Richardson number (left) and the buoyancy flux (right).

higher and broader peaks, or they decay in amplitude and disappear amplifying the adjacent peaks(Figure 14(top)). The flux on the other hand, started from an initial condition which has a weak constant value within the interior and after the instabilities have developed its value also remained constant, however at a higher value (Figure 14(bottom)). Note that the merging and decaying events are accompanied by a transient decrease in buoyancy flux. This is clearly seen at Figure13, where, for example, the two peaks at $z \approx 550$ or $z \approx 750$ are about to merge and the corresponding values of the buoyancy flux are decreased. The edge regions which are characterized by weak stratification and buoyancy flux are continuously growing free of instabilities. The end result of such a simulation would be the full homogenization of the buoyancy, since system is forced by the mean flow which is a continuous source of turbulent mixing.

The numerical simulation, showed that a series of mixed layers could form in a region subjected to the action of the mean flow turbulence. However, the simulation was performed in an idealized setting so that it could confirm the results of the linear analysis of the stability of the model. The model only conceptually shows the mechanism of layer formation. In reality, there are many more factors that would contribute to the evolution of the layers. First of all, the mixing model uses constant characteristic shear and the mean flow as a mechanisms for the generation of turbulence. However, the mean flow is affected by changes in stratification and should be accounted by the model if the instabilities develop at a similar time scale as the variations in mean flow. Furthermore, in the experiments there is a nonuniform buoyancy gradient profile, as it has a dominant peak at the base of the primary mixed layer. The existence of this layer affects the evolution of the adjacent secondary mixed layers. Nonetheless, the model shows the important features of the evolution of the secondary mixed layers: spontaneous generation of the layers, the merging of the layers and their decay - all of which have been observed in the experiments. Even though the proposed model simulates similar behavior to the observations, the assumption of the model should be verified experimentally - this would require elaborate measurements of the mean flow as well as the of the turbulent buoyancy and momentum fluxes.

4 Conclusions

A series of experiments were performed on a linearly stratified fluid subjected to the surface frictional stress induced by a rotating disk. The control parameters for the experiments were the magnitude of the stratification (N^2) and the rotating speed of the disk (Ω) resulting in a single non-dimensional parameter $Ri = N^2/\Omega^2$. Two types of mixed layers have been observed - the primary layer extending from the surface into the interior of the fluid, and the secondary mixed layer of much smaller scale that forms underneath it. The growth of the primary layer with time seems to obey a power law $\hat{h} \sim Ri^{-1/3}\hat{t}^{2/9}$. This result is consistent with the energy balance model that assumes a constant kinetic energy withing the layer.

The secondary mixed layers show a complicated behavior, having several regimes depending on time and the Richardson number of the experiment. A physical mechanism for the formation of the secondary mixed layers has not been clearly identified from the observations due to the lack of observational data, namely the turbulent fluxes and the mean flow. Nonetheless, the hypothesis has been put forward that relates the formation of these layers to an instability of the flux-gradient type that could arise in stratified turbulent flows. A one dimensional mixing model has been devised and the instabilities were investigated theoretically as well as through numerical simulations. The resulting mixed layers form only in a particular regime that puts constraints on the magnitude of the mean flow with respect the its shear and the Richardson number for the profile. Furthermore, the dynamics predicts the destruction of the mixed layers through merging and decay - the precesses observed in experiments.

Based on the mixing model, the results of the experiments could be interpreted as follows. Supported by the disk generated turbulence, the primary mixed layer grows creating a large density gradient at the base of it. At the same time, the mean flow is established within the primary layer. The flow is suppressed as it reaches high stratification and thus the shear is created at the base of the mixed layer. This sets a particular value of the model parameter Q, which reflects the relative importance of the mean flow to the mean shear. The magnitude of the flow as well as of its shear changes with time as the mixed layer grows, meaning that Q is a function of time as well as space. The formation of the secondary mixed layers below the primary is observed when the necessary conditions for the instabilities are met: the parameter Q is smaller then the critical value, and the local Richardson numbers belong to the unstable part of the flux-gradient curve. Such a constrain identifies a confined region in a fluid where the instabilities could occur. The instabilities within this region lead to the development of the layers, however the magnitude of the instabilities is suppressed by the stabilizing effect of the mean flow turbulence. That explains why secondary mixed layers are not completely destratified. After the spontaneous development of the layers, comes the stage of slow evolution when the layers either merge with the primary interface of decay by erosion - consistent with the behavior of the observed layers. The change in the regime is the shift from the dominating collision instability to the erosion instability which is associated with the change in the base state.

Acknowledgements

The present study was conducted under the Geophysical Fluid Dynamics Program at Woods Hole Oceanographic Institution. I would like thank Colm Caulfield for advising me on this project and Niel Balmforth for many productive discussions. All the lectures for giving excellent presentations on modern topics of fluid dynamics. And a special thanks to the fellows for the friendly atmosphere and overnight discussions that made this program a unique and unforgettable experience.

References

[1] N. Balmforth, S. Smith, and W. Young, *Dynamics of interfaces and layers in a stratified turbulent fluid*, Journal of Fluid Mechanics, 355 (1998), pp. 329–358.

[2] G. Barenblatt, M. Bertsch, R. Passo, V. Prostokishin, and M. Ughi, *A mathematical model of turbulent heat and mass transfer in stably stratified shear flow*, Journal of Fluid Mechanics, 253 (1993), pp. 341–358.

[3] P. Davies, Y. Guo, D. Boyer, and A. Folkard, *The flow generated by the rotation of a horizontal disk in a stratified fluid*, Fluid Dynamics Research, 17 (1995), pp. 27–47.

[4] H. Fernando, *Turbulent mixing in stratified fluids*, Annual review of fluid mechanics, 23 (1991), pp. 455–493.

[5] G. Oster and M. Yamamoto, *Density Gradient Techniques.*, Chemical Reviews, 63 (1963), pp. 257–268.

[6] Y. Park, J. Whitehead, and A. Gnanadeskian, *Turbulent mixing in stratified fluids: layer formation and energetics*, Journal of Fluid Mechanics, 279 (1994), pp. 279–311.

[7] O. Phillips, *Turbulence in a strongly stratified fluid -is it unstable?*, in Deep Sea Research and Oceanographic Abstracts, vol. 19, Elsevier, 1972, pp. 79–81.

[8] E. Posmentier, *The generation of salinity finestructure by vertical diffusion*, Journal of Physical Oceanography, 7 (1977), pp. 298–300.

[9] T. Radko, *Mechanics of merging events for a series of layers in a stratified turbulent fluid*, Journal of Fluid Mechanics, 577 (2007), pp. 251–273.

[10] J. Simpson and J. Woods, *Temperature microstructure in a fresh water thermocline.*, Nature, 226 (1970), p. 832.